Kinetics of Nonisothermal Polymer Crystallization

Jiao Yang and Benjamin J. McCoy†

Department of Chemical Engineering, Louisiana State University, Baton Rouge, Louisiana 70803

Giridhar Madras*

Department of Chemical Engineering, Indian Institute of Science, Bangalore 560 012, India

Received: April 29, 2005; In Final Form: July 8, 2005

We adopt a cluster size distribution model to investigate the kinetics of nonisothermal polymer crystallization. The time dependencies of polymer concentration, number and size of crystals, and crystallinity (in Avrami plots) are presented for different cooling rates. The incubation period is also investigated at different cooling rates and initial temperatures. The relationship between cooling rates and incubation time is presented graphically and compared with experimental measurements. The initial temperature (relative to melting point) has a significant effect on nonisothermal crystallization. A comparison of moment and numerical solutions of the population balance equations shows the influence of Ostwald ripening. Agreement between modeling results and experimental measurements at different cooling rates supports the application of the distribution kinetics model for nonisothermal crystallization.

Introduction

Experimental and modeling studies of polymer crystallization have often been carried out under idealized conditions of constant temperature. A polymer sample is melted at or above the equilibrium melting point, and is rapidly quenched to the temperature chosen for crystallization. In practice, however, industrial processes and some experimental studies generally proceed under dynamic and nonisothermal conditions, in which the crystallization rate depends not only on the instantaneous temperature but also on the rate of temperature change. Because the thermal history experienced by the polymer sample is critical in the determination of the final product properties, an understanding of nonisothermal crystallization is necessary. This is the motivation for extending isothermal crystallization kinetics to nonisothermal conditions.

The overlapping of primary nucleation and crystal growth complicates the kinetics of polymer crystallization,[1−3] ensuring that a fairly sophisticated model will be required. The first attempt to describe the kinetics of polymer crystallization was made by Evans[4] via statistical considerations, and by Avrami[5−7] via the concept of so-called extended volume. Avrami derived the well-known expression for crystallinity as a function of time

$$X(t) = 1 - \exp[-V(t)] \qquad \text{(I)}$$

where $V(t)$ is the extended volume, denoting the total volume of all domains growing from all nucleation attempts occurring at time t. For isothermal crystallization, the Avrami equation simplifies to

$$X(t) = 1 - \exp(-Kt^m) \qquad \text{(II)}$$

where K is a rate coefficient depending on both nucleation and crystal growth rate, and m assumes the values of 1, 2, 3, and 4 depending on the nucleation type and the crystal dimensionality.[8] For years the kinetic analysis for polymer crystallization has involved plots based on the Avrami equation, even though it was often criticized as being oversimplified.[8−10] Although the empirical basis of eq II allows it to describe some fundamental features of crystallization, the exponent value m, determined experimentally for various polymers (mainly on the basis of DSC measurements of latent heat during crystallization), is rarely in agreement with the predicted integer numbers.[11−14] A number of authors[15−17] also pointed out that the Avrami plot of experimental measurements, $\log[-\ln(1 - X)]$ vs $\ln(t)$, is actually a curved rather than straight line proposed by the Avrami theory. These observations suggest that the assumptions leading to the Avrami equation are simplistic, and that its foundation is inexact.

Neither eq I nor II can be used directly in nonisothermal crystallization unless the temperature dependence of $V(t)$ or K is known. Nonisothermal crystallization has been modeled by applying a linear temperature change to the Avrami equation.[18−21] To evaluate kinetic parameters, the Tobin[22] and Ozawa[19] models allowed K to depend on the cooling rate. Taking into account the transient and nonisothermal effects, Ziabicki[23,24] proposed a new model for polymer crystallization in which external variables, such as temperature, pressure, and stress, change in time. Generalized equations for polymer crystallization under variable external conditions were developed by introducing three temperature-dependent material functions: steady-state crystallization rate, relaxation time, and isothermal nucleation. Experimental studies of nonisothermal crystallization at cooling rates between 2 and 40 °C/min with the DSC method[20] showed an increase in the Avrami exponent as the cooling rate increased. The effect of the cooling rate on the crystallinity[9] indicated that the Avrami equation could not quantitatively describe nonisothermal crystallization, and required an additional compensating parameter. The mathematical description of the spherulitic pattern formation in nonisothermal conditions was elaborated

* Corresponding author. Phone: 91-080-2293-2321. Fax: 91-080-2360-0683. Email: giridhar@chemeng.iisc.ernet.in.

† Current address: Department of Chemical Engineering & Materials Science, University of California, Davis, CA 95616.

10.1021/jp052219b CCC: $30.25
Published on Web 09/13/2005

on the basis of the assumption of the momentary randomness of primary nucleation.[25−27] This probabilistic approach makes it possible to describe the formation of spherulitic structural elements in the course of nonisothermal crystallization. The temperature dependencies of the material functions are still uncertain, however, and the Avrami exponent for nonisothermal crystallization requires further investigation.

The Avrami equation, with its basis in heuristic ideas, is still applied to polymer crystallization, even though the controversy about the underlying mechanism has continued since the derivation of this equation. This leads us to propose a new cluster distribution model for polymer crystallization kinetics by considering the similarity between crystal growth and monomer deposition on clusters.[2,3] Based on the fundamental concepts of nucleation and crystal growth, the model accounts for homogeneous or heterogeneous nucleation and crystal growth for isothermal crystallization. The model proved capable of quantitatively describing experimental data for isothermal polymer crystallization. In the current paper, we will investigate nonisothermal crystallization kinetics with linear cooling rates. The temperature effect is incorporated into the model by the temperature dependencies of the interfacial energy, equilibrium solubility, and growth rate coefficient.

Theory

We hypothesize that polymer crystal growth is similar to the deposition of molecules on clusters. This deposition process by which polymer molecules of mass $x' = x_m$ are reversibly attached or dissociated from an established crystal of mass x can be represented as a reaction-like process[28]

$$\mathrm{C}(x) + \mathrm{M}(x_m) \underset{k_d(x)}{\overset{k_g(x)}{\rightleftharpoons}} \mathrm{C}(x + x_m) \tag{1}$$

where C(x) represents the crystal of mass x and M($x' = x_m$) is the macromolecule with a uniform molecular weight distribution written in terms of monomer concentration $m^{(0)}(t)$ and monomer molecular weight x_m, as $m(x, t) = m^{(0)}(t)\,\delta(x - x_m)$. The mass-dependent rate coefficients $k_g(x)$ and $k_d(x)$ are for cluster growth and dissociation, respectively. An activation energy, E, is assumed to account for the temperature dependence of the growth rate coefficient, $k_g(x) = \gamma x^{\lambda} \exp(-E/RT)$ where γ is a temperature-independent constant. Exponent λ accounts for the mass dependence of the growth rate coefficient, representing surface-independent, diffusion-controlled, and surface-dependent growth, respectively, when λ equals 0, 1/3, and 2/3.

Temperature influences crystal growth through kinetics and thermodynamics. The activation energy for the growth rate coefficient accounts for the temperature effects through kinetics, whereas the temperature dependence of the equilibrium solubility for a flat surface

$$m_{\infty}^{(0)} = \mu_{\infty} \exp(-\Delta H/RT) \tag{2}$$

accounts for the temperature influence through thermodynamics. Here, ΔH is the molar enthalpy of the phase transition and μ_{∞} represents the flat-surface equilibrium solubility at high temperature. For a lamellar crystal with a flat growth front, the Gibbs−Thomson effect vanishes, so that the difference between the local equilibrium interfacial concentration $m_{eq}^{(0)}$ and the solubility $m_{\infty}^{(0)}$ for a flat surface vanishes, thus $m_{eq}^{(0)} = m_{\infty}^{(0)}$. The rate coefficient for growth and the dissociation rate coefficient are related, $k_d(x) = m_{eq}^{(0)} k_g(x)$, by microscopic reversibility.[29] Nucleation, the initiation of crystal nuclei, occurs simultaneously with crystal growth. By including the nucleation term, the kinetics of polymer crystallization can be described by the cluster size distribution equations[30]

$$\partial c(x, t)/\partial t = -k_d(x)\, c(x, t) + \int_x^{\infty} k_d(x')\, c(x', t)\, \delta(x - (x' - x_m))\, dx' - k_g(x)\, c(x, t)\, m^{(0)}(t) \int_0^{\infty} \delta(x' - x_m)\, dx' + m^{(0)} \int_0^{x} k_g(x')\, c(x', t)\, \delta(x - x_m)\, dx' + I\delta(x - x^*) \tag{3}$$

and

$$\partial m(x, t)/\partial t = -m^{(0)}(t) \int_0^{\infty} k_g(x')\, c(x', t)\, dx' + \int_x^{\infty} k_d(x')\, c(x', t)\, \delta(x - x_m)\, dx' - I\delta(x - x^*)\, x^*/x_m \tag{4}$$

where x^* represents the critical crystal mass and I denotes nucleation rate. For a supersaturated (metastable) system, the cluster energy of a crystal of radius r reaches a maximum value at the critical crystal radius. According to classical nucleation theory,[31,32] the nucleation rate (moles of nuclei per vol per time) is the flux over the maximum energy barrier at the critical radius

$$I = k_n \exp(-W^*/RT) \tag{5}$$

where W^* represents the energy barrier for the nucleation of crystal with critical mass x^*, and the nucleation prefactor written in terms of crystal density, ρ, and crystal interfacial energy, σ, is

$$k_n = (m^{(0)})^2 (2\sigma x_m/\pi)^{1/2} \rho^{-1} \tag{6}$$

The classical nucleation theory utilizes the sum of the surface energy and the formation free energy; for an equilateral lamellar crystal of characteristic length a

$$W(a) = 4ab\sigma - a^2 b(\rho/x_m) RT \ln S_{sat} \tag{7}$$

where b is the thickness of the lamellar crystal and σ is the crystal interfacial energy with its temperature dependence approximated as[3,33]

$$\sigma = \sigma_0 (1 - T/T_m)^n \tag{8}$$

where n and σ_0 are constants dependent on the polymer. The equation indicates that the interfacial energy σ vanishes at reference temperature T_m. The chemical potential difference ($-RT \ln S_{sat}$) between the two phases is expressed in terms of supersaturation S_{sat}, which is the ratio of bulk monomer concentration $m^{(0)}$ over the equilibrium monomer concentration $m_{eq}^{(0)}$. The maximum energy occurs at the critical crystal size

$$a^* = 2\sigma x_m/(\rho RT \ln S_{sat}) \tag{9}$$

which can be converted into critical crystal mass. Thus the nucleation energy barrier, according to eq 7, is

$$W^* = 4x_m b\sigma^2/[\rho RT \ln(m^{(0)}/m_{eq}^{(0)})] \tag{10}$$

With the definitions of dimensionless quantities in our previous work[3] we may write the cluster size distribution

$$C = cx_m/\mu_{\infty},\ C^{(n)} = c^{(n)}/\mu_{\infty} x_m^{\,n},\ \xi = x/x_m,\ \theta = t\gamma\mu_{\infty} x_m^{\,\lambda},\ S = m^{(0)}/\mu_{\infty},\ \Theta = T/T_m,\ w = 2\sigma_0 (x_m b/\rho)^{1/2}/RT_m,\ J = I/\gamma\mu_{\infty}^{\,2} x_m^{\,\lambda},\ \epsilon = E/RT_m,\ h = \Delta H/RT_m \tag{11}$$

equations in dimensionless form

$$dS(\theta)/d\theta = \exp(-\epsilon/\Theta)[-S(\theta) + \exp(-h/\Theta)]C^{(\lambda)} + J\xi^* \quad (12)$$

and

$$\partial C(\xi, \theta)/\partial\theta = S(\theta)\exp(-\epsilon/\Theta)(-\xi^{\lambda}C(\xi, \theta) + (\xi - 1)^{\lambda}C(\xi - 1, \theta)) - \xi^{\lambda}\exp(-(\epsilon + h)/\Theta)C(\xi, \theta) + (\xi + 1)^{\lambda}\exp(-(\epsilon + h)/\Theta)C(\xi + 1, \theta) - J\delta(\xi - \xi^*) \quad (13)$$

The initial conditions are $S(\theta = 0) = S_0$ and $C(\xi, \theta = 0) = 0$, where ξ is defined as the number of macromolecules in the crystal. The source term $J\delta(\xi - \xi^*)$ represents the scaled nucleation rate of crystals having ξ^* macromolecules. The number of macromolecules in the critical crystal nucleus is

$$\xi^* = [w(1 - \Theta)^n/\Theta \times (\ln S + h/\Theta)]^2 \quad (14)$$

which varies with time, because of the time dependence of the scaled number of crystallizing polymers S, and is strongly dependent on temperature. When ripening occurs, a sink term appears representing the denucleation of crystals smaller than the critical size. By defining the temperature-independent prefactor, $J_0 = (2\sigma_0/\pi)^{1/2}/\rho\gamma x_m^{\lambda-1/2}$, the nucleation rate can be written as

$$J = J_0(1 - \Theta)^{n/2} S^2 \exp[-(w(1 - \Theta)^n/\Theta)^2/(\ln S + h/\Theta)] \quad (15)$$

With the definition of the jth moment, $C^{(j)} = \int_0^\infty \xi^j C(\xi,\theta)\, d\xi$, the dimensionless cluster size distribution equations, for the special case $\lambda = 0$, can be rewritten as moment equations

$$dC^{(0)}(\theta)/d\theta = J \quad (16)$$

and

$$dC^{(1)}(\theta)/d\theta = -\exp(-\epsilon/\Theta)[-S(\theta) + \exp(-h/\Theta)]C^{(0)} - J\xi^* \quad (17)$$

The zeroth moment, $C^{(0)}$, and the first moment, $C^{(1)}$, represent the time-dependent molar (number) and mass concentrations of crystal, respectively. The ratio of the two moments is the average size of the crystals, $C^{avg} = C^{(1)}/C^{(0)}$. In terms of the initial number of polymer molecules S_0, the scaled mass conservation for a closed system follows from the population balance equations, eqs 12 and 17

$$C^{(1)}(\theta) + S(\theta) = C_0^{(1)} + S_0 \quad (18)$$

where $C_0^{(1)}$ is the initial cluster mass and is zero for homogeneous nucleation and S_0 is the initial number of polymer molecules.

To use eqs 13−15 in the analysis of nonisothermal crystallization, it is assumed that the polymer sample experiences a constant cooling rate. Though we adopt a linear decrease of temperature with time, one can easily incorporate any variation of temperature with time in the model. The relationship between crystallization time t and the crystallization temperature T is thus

$$T = T_0 - \beta t \quad (19)$$

where β is the cooling rate (K/min) and T_0 is the initial temperature. With the dimensionless quantities $\theta = t\gamma\mu_\infty x_m^{\lambda}$ and $\Theta = T/T_m$, where temperatures are represented in Kelvins, the relationship can be rewritten as

$$\Theta = \Theta_i - \phi\theta \quad (20)$$

where $\Theta_i = T_0/T_m$ is the dimensionless initial temperature and $\phi = \beta/[\gamma\mu_\infty T_m x_m^{\lambda}]$ is the dimensionless cooling rate. Thus eqs 12, 16, and 17, for the crystallization in which a polymer sample is cooled from its melting point, T_m, can be rewritten in terms of dimensionless time θ

$$dS(\theta)/d\theta = \exp(-\epsilon/(1 - \phi\theta))[-S(\theta) + \exp(-h/(1 - \phi\theta))]C^{(0)} + J\xi^* \quad (21)$$

$$dC^{(0)}(\theta)/d\theta = J \quad (22)$$

and

$$dC^{(1)}(\theta)/d\theta = -\exp(-\epsilon/(1 - \phi\theta))[-S(\theta) + \exp(-h/(1 - \phi\theta))]C^{(0)} - J\xi^* \quad (23)$$

Based on eq 20, eqs 21−23 can be rewritten in terms of temperature Θ

$$dS(\Theta)/d\Theta = -(1/\phi)[\exp(-\epsilon/\Theta)[-S(\Theta) + \exp(-h/\Theta)]C^{(0)} + J\xi^*] \quad (24)$$

$$dC^{(0)}(\Theta)/d\Theta = -(1/\phi)J \quad (25)$$

and

$$dC^{(1)}(\Theta)/d\Theta = -(1/\phi)[-\exp(-\epsilon/\Theta)[-S(\theta) + \exp(-h/\Theta)]C^{(0)} - J\xi^*] \quad (26)$$

The degree of crystallinity X is defined as the ratio of polymer crystallized at time θ over the total crystallized polymer mass

$$X = (C^{(1)} - C_0^{(1)})/(C_{eq}^{(1)} - C_0^{(1)}) \quad (27)$$

Substitution of the mass conservation equation, eq 18, simplifies eq 27 to

$$X = (S_0 - S(\theta))/(S_0 - e^{-h/\Theta}) \quad (28)$$

Thus the crystallinity time or temperature dependence of crystallinity can be obtained by solving the above ordinary differential moment equations with various cooling rates, ϕ.

Results and Discussion

For the non-steady-state nonisothermal polymer crystallization, our general concern is the effect of the cooling rate on the cluster size distribution. On the basis of the relationship between temperature and time, eq 19, we investigated the cluster size distribution as a function of temperature and time, respectively, as shown in eqs 21−26. Our choice of parameters is based on earlier papers,[2,3] for example, eq 8, proposed in our previous work with suggested values of n,[3] and is used to present the temperature dependence of interfacial energy. The interfacial energy parameter, w, written in terms of density, is chosen to be $w = 2$ in our computation. The molar enthalpy of phase transition, h, is usually around 100. The activation energy for growth rate, ϵ, is typically smaller than h, and a value $\epsilon = 1.0$ is chosen. The homogeneous nucleation rate is very sensitive to supersaturation S_{sat} and temperature, and a constant nucleation rate prefactor, $J_0 = 10^6$, is proposed. We assume the polymer melt is cooled from the melting temperature, $\Theta_i = 1$, where

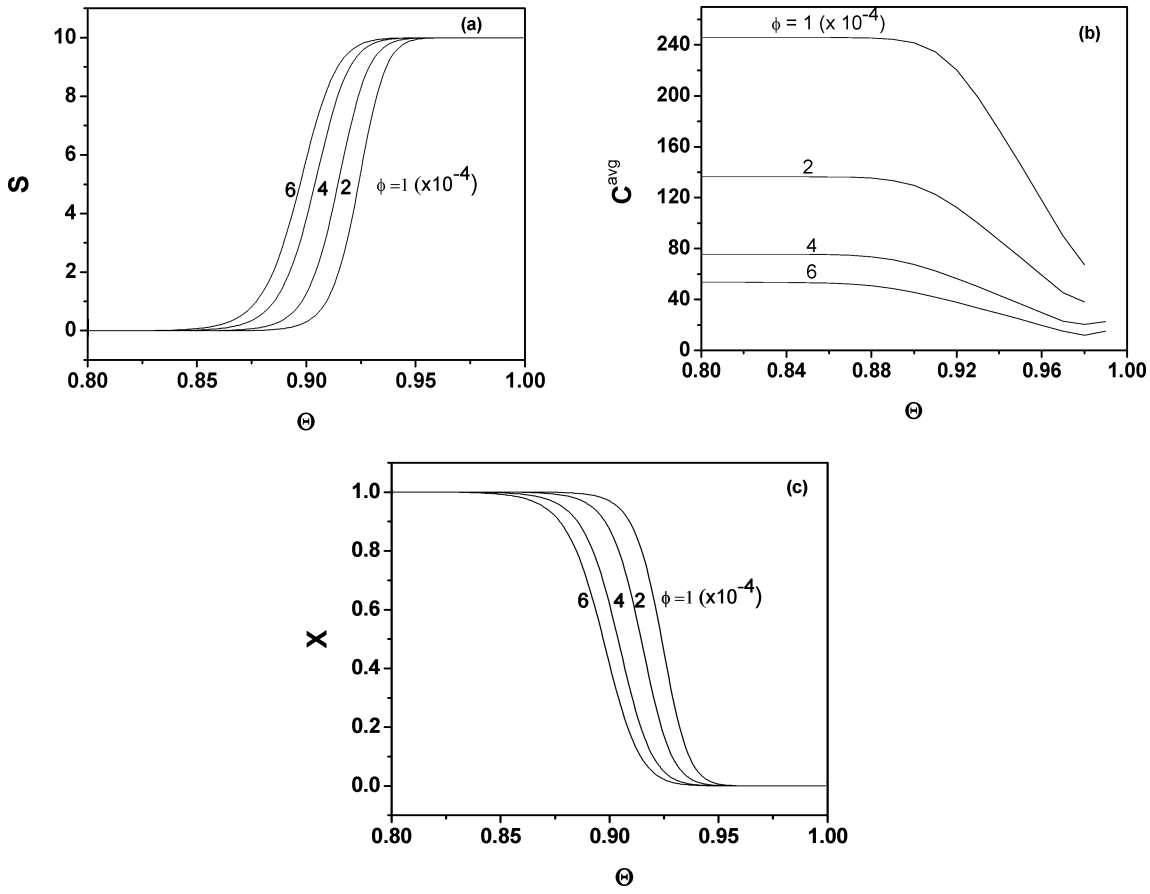

Figure 1. Distribution properties. (a) Supersaturation, (b) average size and (c) relative crystallinity as a function of scaled temperature at different cooling rates, with $C_0^{(0)} = 0$, $C_0^{(1)} = 0$, $S_0 = 10$, $\epsilon = 1.0$, $h = 100$, $n = 20$, $w = 2.0$, $J_0 = 10^6$, $\lambda = 0$, and $\Theta_i = 1$.

the subscript i denotes the initial condition. There are no particles present initially for homogeneous nucleation; thus the initial conditions are $S(\Theta = \Theta_i) = S_0$, $C^{(0)}(\Theta = \Theta_i) = 0$, and $C^{(1)}(\Theta = \Theta_i) = 0$.

The temperature dependence of crystal size distribution is presented in Figure 1 at different cooling rates. The dimensionless cooling rate ϕ varies from 10^{-4} to 6×10^{-4}. Figure 1a presents the effect of cooling rate on the evolution of the number of macromolecules, S, which decreases sharply as temperature drops. The effect of the cooling rate on the crystal size is presented in Figure 1b, in which an increased cooling rate diminishes the average crystal size. This can be explained by the formation of more nuclei as the temperature decreases at a large cooling rate. The extent of crystallization[2,3] is denoted by relative crystallinity, $X = (S_0 - S(\Theta))/(S_0 - e^{-h/\Theta})$, presented in Figure 1c as a function of temperature at different cooling rates. A sharp increase of crystallinity occurs after a short incubation time. According to the definition of crystallinity, $S(\Theta)$ and $X(\Theta)$ are mirror images.

According to eqs 21−23, the crystal size distribution can also be presented as a function of time. Figure 2 presents the time evolution of nonisothermal crystallization of PTT (poly(trimethylene terephthalate))[34] starting from the melting temperature, $\Theta_i = 1$. Figure 2a presents the time evolution of S at different cooling rates. We notice that the decrease of S is delayed by the increasing induction times at smaller cooling rates. The induction time prediction, not present for isothermal crystallization,[3] but occasionally reported in nonisothermal measurements,[12,13] supports the current model. The average crystal size, pictured in Figure 2b for different cooling rates, increases sharply and finally reaches a constant limit. The final crystal size is also controlled by the cooling rate: a large average crystal size is caused by a small cooling rate. This can be explained by the temperature dependence of nucleation; when the cooling rate is small, nucleation and growth occur within a temperature region closer to the reference temperature where the nucleation rate is small. Time evolution of crystallinity is presented in Figure 2c. The conventional Avrami plot of $\log[-\ln(1 - X)]$ vs $\ln(t)$ is presented in Figure 2d. A constant asymptote at the end of crystallization is observed as in isothermal crystallization. The straight midportion of the Avrami plot represents nucleation and growth in which denucleation and ripening are negligible. The Avrami exponent, the slope of this straight portion of the Avrami plot, has little dependence on the cooling rates as the polymer sample is cooled from the melting temperature.

All the crystallinity curves (Figure 2c) include the incubation time $\Delta\theta_{inc}$, defined as a time period from initial temperature, Θ_i, to the onset temperature, Θ_{onset}, where the polymer melt actually begins to crystallize. Thus the incubation period[34] is formulated as $\Delta\theta_{inc} = (\Theta_i - \Theta_{onset})/\phi$. We define the crystallization onset temperature, Θ_{onset}, as the temperature when the crystallinity reaches 1% in the numerical modeling results.

The incubation period, Δt_{inc}, is calculated by quantifying the physical properties of the polymer[35] ($\Delta H = 28.8$ kJ/mol). The melting temperature, T_m, for PTT is reported[34] as 548 K (275 °C). The dimensionless cooling rates, ϕ, are converted into real cooling rates, β, according to $\phi = \beta/(\gamma\mu_\infty T_m x_m^\lambda)$. Thus with $\lambda = 0$, $\gamma\mu_\infty = \beta/(T_m\phi)$ and is 27.36 min^{-1}. The dimensionless incubation time, $\Delta\theta_{inc}$, determined from the moment evaluation of the kinetics model, is converted into a real incubation period, Δt_{inc}, according to eq 11. With $\lambda = 0$, $\gamma\mu_\infty = 27.36$ min^{-1}, Δt_{inc} (min) $= \Delta\theta_{inc}/(\gamma\mu_\infty) = 0.03655\Delta\theta_{inc}$. The calculated

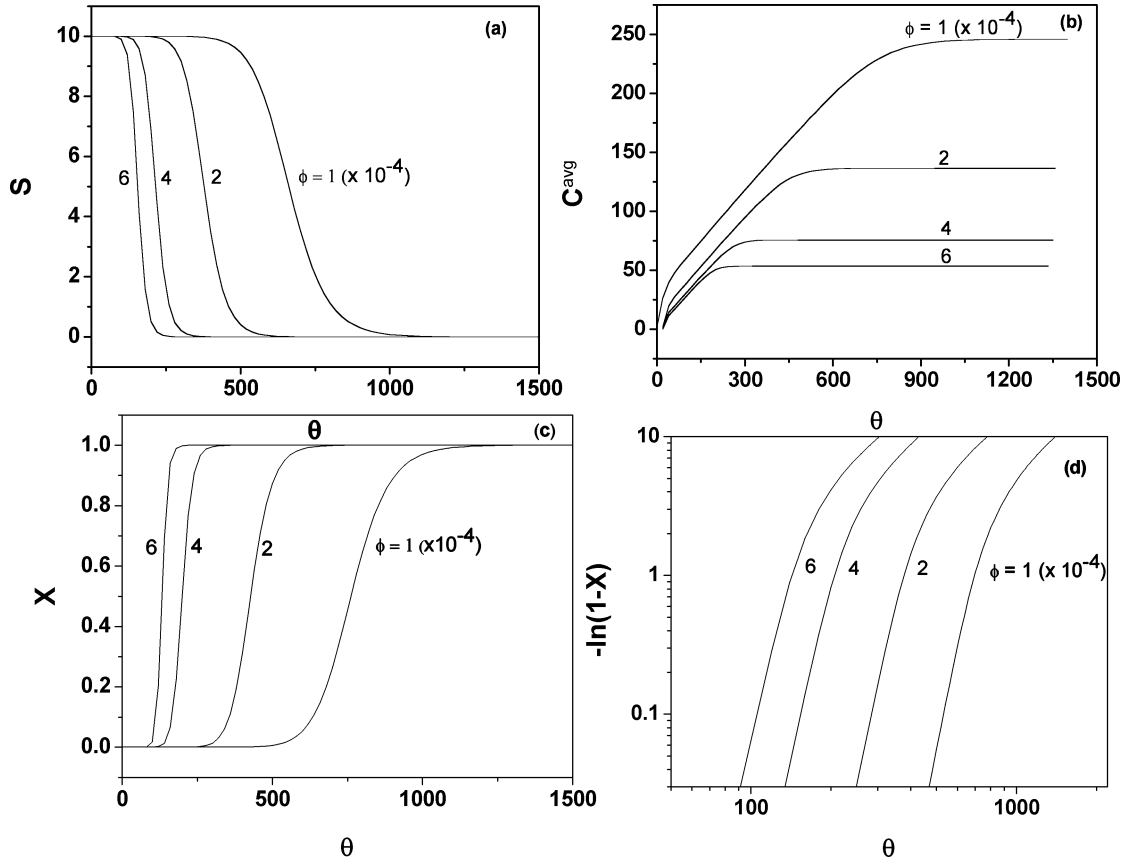

Figure 2. Time evolution of S, C^{avg}, crystallinity, and the conventional Avrami plot for nonisothermal crystallization of PTT at different cooling rates, with $C_0^{(0)} = 0$, $C_0^{(1)} = 0$, $S_0 = 10$, $\epsilon = 1.0$, $h = 100$, $n = 20$, $w = 2.0$, $J_0 = 10^6$, $\lambda = 0$, and $\Theta_i = 1$.

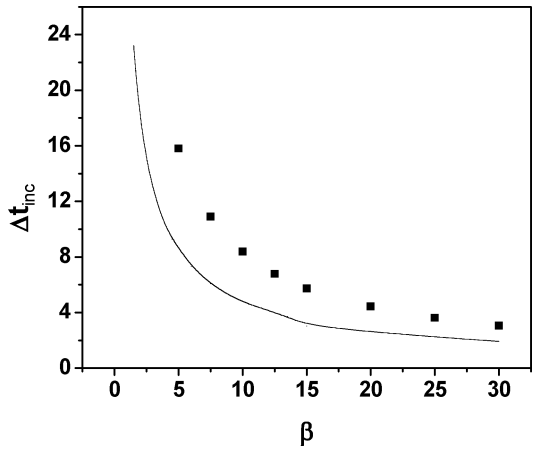

Figure 3. Effect of the cooling rate on the incubation time for nonisothermal crystallization of PTT: (■) experimental measurements,[34] (—) simulation results, with $C_0^{(0)} = 0$, $C_0^{(1)} = 0$, $S_0 = 10$, $\epsilon = 1.0$, $h = 100$, $n = 20$, $w = 2.04$, $J_0 = 10^6$, $\lambda = 0$, and $\Theta_i = 1$.

TABLE 1: Calculated Incubation Period at Different Cooling Rates with $\Theta_i = 1$

scaled cooling rate $\phi(10^{-4})$	real cooling rate β (°C/min)	scaled incubation time $\Delta\theta_{inc}$	real incubation time Δt_{inc} (min)
1	1.5	633.5	23.2
2	3	356	13.0
3	4.5	236.5	8.6
5	7.5	166	6.1
7	10.5	103	3.8
10	15	93.5	3.4
20	30	52.5	1.9

incubation times at different cooling rates are listed in Table 1 for the crystallization of PTT.

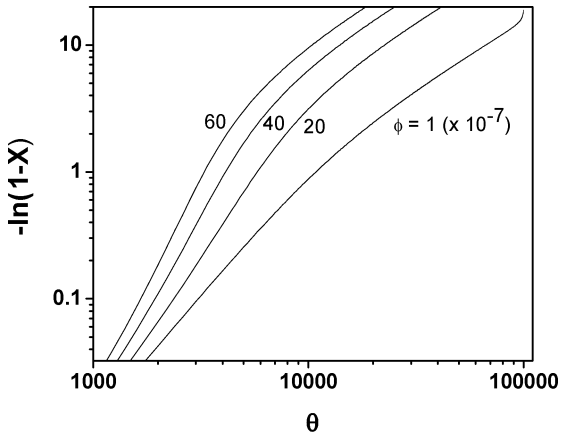

Figure 4. Avrami plots showing the effect of the cooling rate for nonisothermal crystallization, with $C_0^{(0)} = 0$, $C_0^{(1)} = 0$, $S_0 = 10$, $\epsilon = 1.0$, $h = 100$, $n = 20$, $w = 2.0$, $J_0 = 10^6$, $\lambda = 0$, and $\Theta_i = 0.97$.

The equation relating ϕ and β provides an adjustable parameter based on material properties. The relationship between increasing cooling rate and decreasing incubation time is presented quantitatively in Figure 3. Experimental measurements of incubation for PTT are also provided (Figure 3) for comparison. The points represent the experimental measurements[34] of incubation time for PTT, and the solid line stands for the incubation period calculated by the distribution kinetics model at different cooling rates. Good agreement is seen between model simulation and experimental results.

Usually nonisothermal crystallization experiments are conducted by decreasing the temperature from the melting point. However, as the onset temperature is below the melting temperature,[34] our model can also represent nonisothermal crystal-

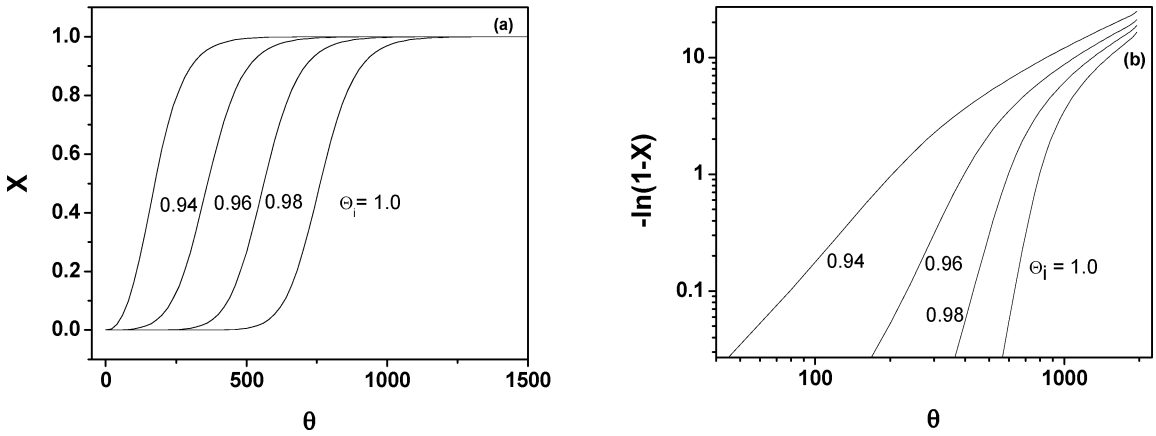

Figure 5. Effect of the initial temperature for nonisothermal crystallization, with $C_0^{(0)} = 0$, $C_0^{(1)} = 0$, $S_0 = 10$, $\epsilon = 1.0$, $h = 100$, $n = 20$, $w = 2.0$, $J_0 = 10^6$, $\lambda = 0$, and $\phi = 1 \times 10^{-4}$. (a) Time evolution of crystallinity X. (b) The conventional Avrami plots at different initial temperatures.

TABLE 2: Calculated Incubation Period at Different Initial Temperatures with $\phi = 4 \times 10^{-4}$

scaled starting temperature Θ_i	real starting temperature T (°C)	scaled incubation time $\Delta\theta_{inc}$	real incubation time Δt_{inc} (min)
1	275.0	520	19.0
0.99	269.5	420	15.4
0.98	264.0	220	8.0
0.97	258.6	130	4.8
0.96	253.1	104	3.8
0.95	247.6	65	2.4
0.94	242.1	30	1.1

lization starting from a temperature below melting. Figure 4 shows the effect of cooling rate when the initial temperature of crystallization is 0.97. Although there is no apparent Avrami exponent change in Figure 2d as the crystallization temperature drops from the melting point, the slope differences for the Avrami plots in Figure 4 indicate a considerable influence of cooling rates as the polymer sample is cooled from a temperature below the melting point. This confirms that the nonisothermal crystallization is sensitively influenced by nucleation, and depends not only on the instantaneous temperature but also on the change rate of temperature, consistent with experimental measurements.[21]

The initial temperature is another influential parameter for nonisothermal crystallization, as shown in Figure 5, which presents time evolution of crystallinity for nonisothermal crystallization starting from different initial temperatures.

The incubation time, increasing as initial temperature increases, reaches a maximum when the polymer melt is cooled from the melting temperature. The incubation periods for different initial temperatures for PTT ($T_m = 275.0$ °C) are listed in Table 2.

Figure 6 presents the dependence of a scaled incubation period on the dimensionless initial temperature, revealing the increase in incubation time with increasing initial temperature. The initial temperature significantly influences the Avrami exponent (Figure 5b), which increases with initial temperature, as shown by the slope increase of the Avrami plots when the initial temperature increases.

The moment method provides an easy and quick solution in modeling polymer crystallization with mass-independent crystal growth ($\lambda = 0$). When the crystal growth rate is mass-dependent ($\lambda > 0$), a more general form, $k_g(x) = \gamma x^\lambda \exp(-E/RT)$, is used to express the crystal growth coefficient. The effect of λ on the crystallization kinetics needs to be explored because it is the most important parameter influencing the Avrami exponent for isothermal crystallization.[3] The moment equations, however, do

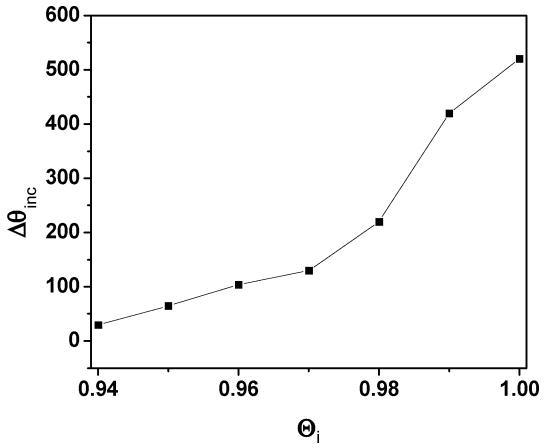

Figure 6. Effect of the initial temperature on the computed incubation time for nonisothermal crystallization. The line segments connect the computed values.

not have a closed form for $\lambda > 0$; thus eqs 12 and 13 were solved at different values of λ by a numerical procedure described in detail in our previous publications.[29,30] A comparison is made between moment and numerical solution for $\lambda > 0$ (Figure 7a). Solid lines and dotted lines represent the numerical solution and the moment solution, respectively. Except for the discrepancy at the end of crystallization, caused by the increasing effect of denucleation and ripening, good agreement is confirmed at various cooling rates. Crystal resizing and ripening can be considered only with the numerical method, and thus we observed a constant asymptote after the straight Avrami plot by numerical solution. This modeling result agrees with experimental observations that the Avrami plot is a curved rather than straight line.[16,17,19] Panels b and c of Figure 7 present the effect of cooling rates on diffusion-controlled ($\lambda = 1/3$) and surface-dependent ($\lambda = 2/3$) crystal growth, respectively. A large overall crystallization rate is caused when the cooling rate increases, as confirmed in the moment solution. A slope increase of 2.7 in the Avrami plots is observed as the cooling rate increases from 10^{-4} to 6×10^{-4}, in agreement with experimental studies.[21] The effect of λ, the exponent of the growth rate coefficient, is presented in Figure 7d. No apparent slope increase for the Avrami plots occurs when λ increases, although the overall crystallization rate rises because of the increasing dependence of the growth rate coefficient on crystal mass. It is important to notice that, different from isothermal crystallization,[3] the effect of changing temperature dominates over the effect of λ because of the sensitivity of the nucleation rate on

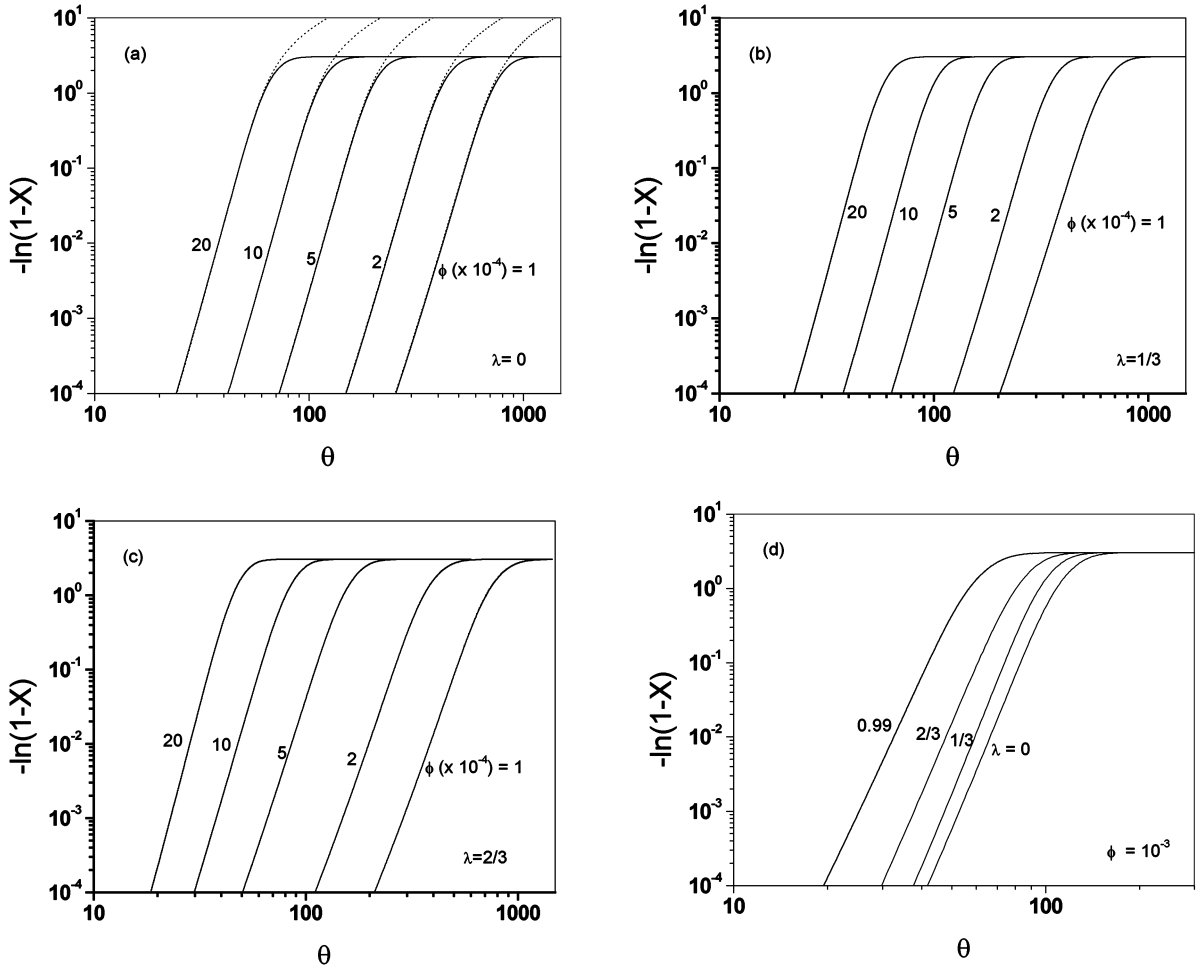

Figure 7. Conventional Avrami plots, with $C_0^{(0)} = 0$, $C_0^{(1)} = 0$, $S_0 = 10$, $\epsilon = 1.0$, $h = 100$, $n = 20$, $w = 2.0$, $J_0 = 10^6$, and $\Theta_i = 1$. The effect of the cooling rate when (a) $\lambda = 0$, (b) $\lambda = 1/3$, and (c) $\lambda = 2/3$. (d) The effect of λ for nonisothermal crystallization with a cooling rate of $\phi = 10^{-3}$. Solid and dotted lines represent the numerical and moment solutions, respectively.

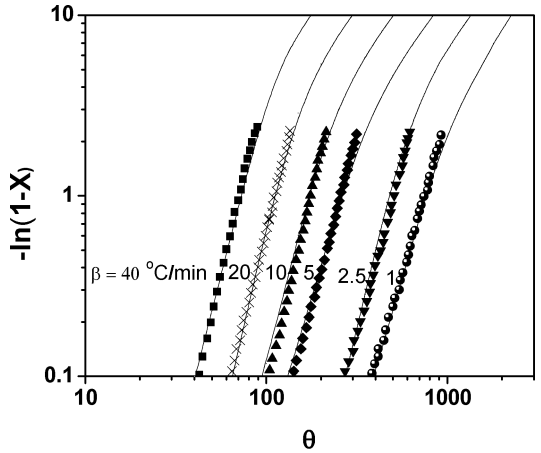

Figure 8. Fits of the cluster size distribution model, with $C_0^{(0)} = 0$, $C_0^{(1)} = 0$, $S_0 = 10$, $\epsilon = 1.0$, $h = 100$, $n = 20$, $w = 2.0$, $J_0 = 10^6$, $\lambda = 0$, and $\Theta_i = 0.96$, to the nonisothermal crystallization measurements[21] for PPT at the following cooling rates (β, °C/min): (■) 40, (×) 20, (▲) 10, (□) 5, (▼) 2.5, (●) 1.

temperature. Thus an apparent slope change in the Avrami plots is not observed for different λ values for nonisothermal crystallization.

To verify the application of the cluster size distribution model to nonisothermal crystallization, we fitted experimental measurements with the model. Figure 8 presents the comparison between simulation results of the model and experimental data[21] for PPT [poly(propylene terephthalate)]. The solid lines represent the model fit, and the points denote the measurements at various cooling rates. A unit transposition is made on the data because our model calculation is based on dimensionless time whereas the experimental data is based on real time. Here a horizontal transposition of $\log(\gamma\mu_\infty x_m^\lambda)$ units ($\gamma\mu_\infty = 125\ \text{min}^{-1}$) is applied to convert the experimental data into plots based on dimensionless time θ.[3] The experimental measurements present the conventional Avrami plots at a cooling rate, β, equal to 1.0, 2.5, 5, 10, 20, and 40 °C/min. Good agreement between experimental and simulation results is observed, indicating a realistic description of nonisothermal crystallization by the crystal size distribution approach.

Conclusion

The crystal size distribution kinetics approach[2,3] applied in the present paper permits an investigation of nonisothermal crystallization. Following our earlier studies on isothermal polymer crystallization,[3] we have investigated the effect of cooling rates in detail for nonisothermal crystallization with linearly decreasing crystallization temperature. The temperature dependencies of crystallinity, supersaturation, and average crystal size are presented for nonisothermal crystallization at different cooling rates. Time evolutions of crystal size distributions are also revealed at different cooling rates. The effect of initial temperature is investigated in detail. An apparent Avrami exponent increase occurs as the initial temperature increases.

The effect of the cooling rate, however, is counteracted by an increasing initial temperature; in other words, increasing the cooling rate has little influence if the crystallization temperature begins from the melting point. The incubation period was also investigated in detail at different cooling rates and different initial temperatures. An increasing incubation period is caused by an increase in the initial temperature or a decrease in the cooling rate. We also investigated the effect of power dependence for growth rate coefficient λ, and did not observe the apparent Avrami exponent increase when the polymer melt was cooled from the melting point, as indicated in isothermal crystallization. The validity of the crystal size distribution model was also examined by comparison with experimental measurements. The model accurately describes the effect of the cooling rate on incubation time and on Avrami plots of crystallinity vs time. Although an analytical, closed expression cannot be derived in our approach, the model and simulation results for the degree of crystallization provide a theoretical foundation for the Avrami plots. That the characteristic Avrami plot for experimental data is curved rather than straight indicates that our approach is capable of providing a more realistic prediction than the oversimplified Avrami theory.

References and Notes

(1) Robson, J. D. *Acta Mater.* **2004**, *52*, 4669.
(2) Yang, J.; McCoy, B. J.; Madras, G. *J. Chem. Phys.* **2005**, *122* (6), 64901.
(3) Yang, J.; McCoy, B. J.; Madras, G. *J. Chem. Phys.* **2005**, *122* (24), 244905.
(4) Evans, U. R. *J . Chem. Soc., Faraday Trans.* **1945**, *41*, 365.
(5) Avrami, M. *J. Chem. Phys.* **1939**, *7*, 1103.
(6) Avrami, M. *J. Chem. Phys.* **1939**, *7*, 212.
(7) Avrami, M. *J. Chem. Phys.* **1939**, *7*, 177.
(8) Hay, J. N. *Polym. Int.* **1971**, *3*, 74.
(9) Wasiak, P.; Sajkiewicz, P.; Wozniak, A. *J. Polym. Sci., Part B: Polym. Phys.* **1999**, *42* (37), 2821.
(10) Piorkowska, E. *J. Phys. Chem.* **1995**, *99*, 14007.
(11) Vilanova, P. C.; Ribas, S. M.; Guzman, G. M. *Polymer* **1985**, *26*, 423.
(12) Xu, J.; Fariclough, J. P. A.; Mai, S. M.; Ryan, A. J.; Chaibundit, C. *Macromolecules* **2002**, *35*, 6937.
(13) Xiao, J.; Zhang, H.; Wan, X.; Zhang, D.; Zhou, Q.; Woo, E. M.; Turner, S. R. *Polymer* **2002**, *43*, 7377.
(14) Ciora, R. J.; Magill, J. H. *Macromolecules* **1990**, *23*, 2350.
(15) Hay, J. N.; Booth, A. *Polym. Int.* **1972**, *4*, 19.
(16) Price, F. P. *J. Appl. Phys.* **1969**, *36*, 3014.
(17) Grenier, D.; Prodhomme, R. E. *J. Polym. Sci., Part B: Polym. Phys.* **1980**, *18*, 1655.
(18) Di Lorenzo, M. L.; Silvestre, C. *Prog. Polym. Sci.* **1999**, *24*, 917.
(19) Ozawa, T. *Polymer* **1971**, *12*, 150.
(20) Kratochvil, J.; Sikora, A. *J. Appl. Polym. Sci.* **2005**, *95*, 564.
(21) Achilias, D. S.; Parageorgiou, G. Z.; Karayannidis, G. P. *J. Polym. Sci., Part B: Polym. Phys.* **2004**, *42*, 3775.
(22) Tobin, M. C. *J. Polym. Sci., Part B: Polym. Phys.* **1976**, *12*, 399.
(23) Ziabicki, A. *Colloid Polym. Sci.* **1996**, *274*, 209.
(24) Ziabicki, A. *Colloid Polym. Sci.* **1996**, *274*, 705.
(25) Piorkowska, E. *J. Phys. Chem.* **1995**, *99*, 14007.
(26) Piorkowska, E. *J. Phys. Chem.* **1995**, *99*, 14016.
(27) Piorkowska, E. *J. Phys. Chem.* **1995**, *99*, 14024.
(28) McCoy, B. J. *J. Phys. Chem. Solids* **2002**, *63*, 1967.
(29) Madras, G.; McCoy, B. J. *Chem. Eng. Sci.* **2004**, *59*, 2753.
(30) Madras, G.; McCoy, B. J. *J. Chem. Phys.* **2002**, *17*, 8042.
(31) McClurg, R. B.; Flagan, R. C. *J. Colloid Interface Sci.* **1998**, *194*, 201.
(32) Oxtoby, D. W. *J. Phys.: Condens. Matter* **1992**, *4*, 7627.
(33) Rowlinson, J. S.; Widom, B. *Molecular Theory of Capillarity*; Oxford University Press: New York, 1982; p 248.
(34) Apiwanthanakorn, N.; Supaphol, P.; Nithitanakul, M. *Polym. Test.* **2004**, *23*, 817.
(35) Chung, W. T.; Yeh, W. J.; Hong, P. D. *J. Appl. Polym. Sci.* **2002**, *83*, 2426.